

## DESIGN HUMAN-ROBOT COLLABORATIVE LIFTING TASK USING OPTIMIZATION

**Asif Arefeen**

Mechanical and Aerospace Engineering  
Oklahoma State University  
Stillwater, Oklahoma 74078, USA

**Yujiang Xiang<sup>1</sup>**

Mechanical and Aerospace Engineering  
Oklahoma State University  
Stillwater, Oklahoma 74078, USA

### ABSTRACT

*In this paper, an optimization-based dynamic modeling method is used for human-robot lifting motion prediction. The three-dimensional (3D) human arm model has 13 degrees of freedom (DOFs) and the 3D robotic arm (Sawyer robotic arm) has 10 DOFs. The human arm and robotic arm are built in Denavit-Hartenberg (DH) representation. In addition, the 3D box is modeled as a floating-base rigid body with 6 global DOFs. The interactions between human arm and box, and robot and box are modeled as a set of grasping forces which are treated as unknowns (design variables) in the optimization formulation. The inverse dynamic optimization is used to simulate the lifting motion where the summation of joint torque squares of human arm is minimized subjected to physical and task constraints. The design variables are control points of cubic B-splines of joint angle profiles of the human arm, robotic arm, and box, and the box grasping forces at each time point. A numerical example is simulated for huma-robot lifting with a 10 Kg box. The human and robotic arms' joint angle, joint torque, and grasping force profiles are reported. These optimal outputs can be used as references to control the human-robot collaborative lifting task.*

Keywords: Motion planning, human-robot interaction, sawyer robot, and inverse dynamic optimization, recursive Lagrangian equation.

### 1. INTRODUCTION

Human-robot lifting is widely used in industry and our daily life. It has greatly improved the productivity and efficiency in the manufacturing industries. In the research field, there is a wide range of interest in human-robot collaboration.

Over the last few decades, researchers developed different biomechanical prediction models for lifting [1-7]. Moreover, there was significant progress in human-robot interaction research. Researchers are now using different learning

techniques for predicting and executing the lifting task successfully. The predictive simulations for collaborative lifting were utilized to study load sharing problems among robots or between human and robot. Sheng et al. [8] proposed a learning framework which combines the imitation learning and reinforcement learning for human-robot table lifting tasks. Evrard et al. [9] presented a probabilistic framework for conducting a human-robot collaborative task with the help of a human operator. DelPreto and Rus [10] provided a real-time interface for human-robot lifting. They have used electromyography (EMG) signals to estimate the human's intention for controlling collaborative object lifting tasks.

This work extends our previous human-human team lifting prediction for the 2D skeleton model [7]. Our goal in this study is to develop a 3D human-robot lifting prediction model to study the human-robot interaction and cause-and-effect. An inverse dynamic optimization formulation is proposed to predict the collaborative lifting motion and hand grasping forces. The human-robot lifting problem is formulated as a nonlinear programming (NLP) optimization problem. The objective function is defined as the summation of joint torque squares for human, which is minimized using an SQP algorithm [11]. The optimization results are reported, including the joint angle, joint torque, and box grasping forces.

### 2. MULTIBODY HUMAN-ROBOT SYSTEM

#### 2.1 Human and box model

A 3D human skeletal arm model and a 3D box are considered in this work, as shown in Figure 1. The human skeletal arm model has  $n_{human} = 13$  DOFs. The box has 6 global DOFs, including three translations and three rotations. The skeletal arm model consists of one physical arm branch and one virtual branch, including the global DOFs. The arm model and the box are constructed by using the robotic formulation of the DH

<sup>1</sup> Contact author: yujiang.xiang@okstate.edu

method [12]. In addition, there are two grasping force vectors ( $\mathbf{f}_1^c$  and  $\mathbf{f}_2^c$ ) acting on the two bottom edges of the box. In this study, human's anthropometric data are generated from GEBOD™ [13], a regression-based utility software based on the measured height, weight, and stature. The DH parameters for the human arm and box model are described in Table 1 and 2, respectively.

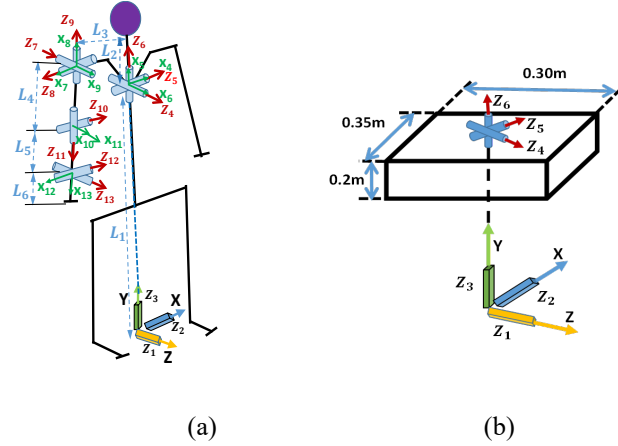


**FIGURE 1:** (a) The 3D human skeletal arm model (with global DOFs:  $z_1, z_2, z_3$ ) and (b) 3D box model (with global DOFs:  $z_1, z_2, z_3, z_4, z_5, z_6$ )

## 2.2 Robotic arm model

A 3D Sawyer robotic arm model is considered in this study, as shown in Figure 2. The model has  $n_{robot} = 10$  DOFs. This arm model has one physical branch and one virtual branch, including three global DOFs. The robotic arm model is constructed using the same DH method.

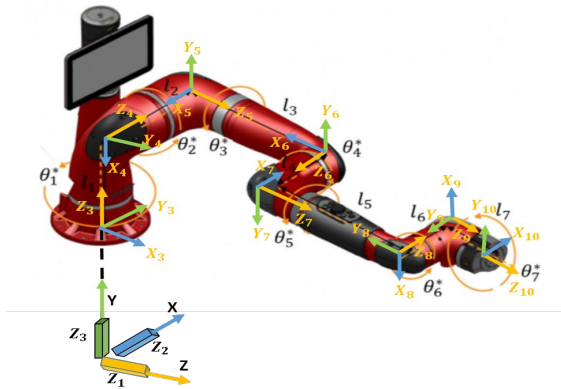


**FIGURE 2.** 3D robotic arm model (Sawyer robotic arm)

The DH parameters for the robotic arm are described in Table 3. The required link lengths of the robotic arm model and the Sawyer robot's link mass data are available in the literature [14]. Recursive Lagrangian dynamics formulation is used to set up the equations of motion (EOM) of the human, robot and box systems, and details refer to [7, 15-16].

Table 1. DH table for human arm model

DOF	$\theta$	$d$	$a$	$\alpha$
1	$\pi/2$	0	0	$\pi/2$
2	$\pi/2$	0	0	$\pi/2$
3	$\pi/2$	$L_1$	0	$\pi/2$
4	$\pi/2$	0	0	$\pi/2$
5	$\pi/2$	0	0	$\pi/2$
6	$-\pi/2$	$L_2$	$L_3$	$-\pi/2$
7	$\pi/2$	0	0	$\pi/2$
8	$-\pi/2$	0	0	$\pi/2$
9	0	$-L_4$	0	$\pi/2$
10	0	0	0	$\pi/2$
11	0	$L_5$	0	$-\pi/2$
12	$\pi/2$	0	0	$-\pi/2$
13	0	0	$-L_6$	0

Table 2. DH table for box model

DOF	$\theta$	$d$	$a$	$\alpha$
1	$\pi/2$	0	0	$\pi/2$
2	$\pi/2$	0	0	$\pi/2$
3	$\pi/2$	0	0	$\pi/2$
4	$\pi/2$	0	0	$\pi/2$
5	$\pi/2$	0	0	$\pi/2$
6	$-\pi/2$	0	0	$-\pi/2$

Table 3. DH table for robotic arm model

DOF	$\theta$	$d$	$a$	$\alpha$
1	$\pi/2$	0	0	$\pi/2$
2	$\pi/2$	0	0	$\pi/2$
3	0	$L_9$	0	0
4	$\pi$	$L_1$	$L_2$	$-\pi/2$
5	$\pi/2$	$L_3$	0	$-\pi/2$
6	0	$L_4$	0	$-\pi/2$
7	$\pi$	$L_5$	0	$-\pi/2$
8	0	$L_6$	0	$-\pi/2$
9	$\pi$	$L_7$	0	$-\pi/2$
10	$-\pi/2$	$L_8$	0	0

## 3. OPTIMIZATION FORMULATION

The human-robot collaborative lifting is predicted by solving an NLP problem. Here the box initial and final positions, the feet/robot base positions, and the box dimensions and weight are given. The total time  $T$  for lifting motion is specified.

### 3.1 Design variables

The joint angle profiles are discretized by cubic B-splines. The design variables ( $\mathbf{x}$ ) are joint angle control points  $\mathbf{P}_{human}$ ,  $\mathbf{P}_{robot}$ , and  $\mathbf{P}_{box}$  for human, robot, and the box, respectively. In addition, the grasping forces ( $\mathbf{f}_1^c$  and  $\mathbf{f}_2^c$ ) between human and

robot, and box are also treated as unknowns (design variables). Thus,  $\mathbf{x} = [\mathbf{P}_{human1}^T, \mathbf{P}_{human2}^T, \mathbf{P}_{box}^T, \mathbf{f}_1^c, \mathbf{f}_2^c]^T$ .

### 3.2 Objective function

The dynamics effort [7,17] is used as the objective function which is defined as the summation of joint torque squares for human.

$$J(\mathbf{x}) = \sum_{i=3}^{n_{human}} \int_0^T \{\tau_{i(human)}^2(\mathbf{P}_{human}, \mathbf{f}_1^c)\} dt \quad (1)$$

where  $T$  is the total time. The total time duration  $T$  is a specified input parameter.

### 3.3 Constraints

The constraints include (i) joint angle limits, (ii) torque limits, (iii) feet/base contacting position, (iv) box forward, (v) box range of motion, (vi) box grasping, (vii) box global EOM, (viii) initial and final box locations, and (ix) static conditions at the beginning and end of the motion. Constraints (i-iv) are imposed for both human and robot, and constraints (v-vii) are imposed only for the box. The physical joint angle limits and joint torque limits for human and robot are depicted in the following equations:

$$\mathbf{q}_{human}^L \leq \mathbf{q}_{human}(t) \leq \mathbf{q}_{human}^U \quad (2)$$

$$\boldsymbol{\tau}_{human}^L \leq \boldsymbol{\tau}_{human}(t) \leq \boldsymbol{\tau}_{human}^U \quad (3)$$

$$\mathbf{q}_{robot}^L \leq \mathbf{q}_{robot}(t) \leq \mathbf{q}_{robot}^U \quad (4)$$

$$\boldsymbol{\tau}_{robot}^L \leq \boldsymbol{\tau}_{robot}(t) \leq \boldsymbol{\tau}_{robot}^U \quad (5)$$

where  $\mathbf{q}_{human}^L$  and  $\mathbf{q}_{robot}^L$  are the lower joint angle limits, and  $\mathbf{q}_{human}^U$  and  $\mathbf{q}_{robot}^U$  are the upper joint limits for the human and robot arm, respectively. In addition,  $\boldsymbol{\tau}_{human}^L$  and  $\boldsymbol{\tau}_{human}^U$  are human dynamic lower and upper joint torque limits, and  $\boldsymbol{\tau}_{robot}^L$  and  $\boldsymbol{\tau}_{robot}^U$  are robot lower and upper limits. Detail formulations of all the constraints are referred to [7].

## 4. RESULTS

An SQP algorithm in SNOPT [11] is used to solve the NLP problem for human-robot lifting. To use the algorithm, cost and constraint functions and their gradients need to be calculated.  $\mathbf{P} = [\mathbf{P}_{human}, \mathbf{P}_{robot}, \mathbf{P}_{box}] = \mathbf{0}$ ,  $\mathbf{f}_1^c = \mathbf{f}_2^c = \mathbf{10}$  are used as the initial guess for the optimization. There are total 224 design variables and 894 nonlinear constraints. The optimal solution is obtained in 141.21 seconds on a laptop with an Intel® Core™ i7 2.11 GHz CPU and 16 GB RAM. The input data to the collaborative box-lifting task include box weight 10 Kg, total time 1.2 seconds, and initial and final box locations. The task parameters are represented in Table 4.

First, the snapshot of the predicted 3D human-robot arm lifting is depicted in Figure 3. The joint angle and joint torque profiles for human shoulder flexion, shoulder abduction, and elbow flexion are shown in Figures 4 and 5, respectively. Similarly, joint angle and joint torque profiles for the robot are

shown in Figures 6 and 7, respectively. Finally, box grasping force profile is presented in Figure 8.

Table 4. Task parameters for the collaborative box lifting

Initial and final human feet contact position (m)	0.375
Initial hand and end-effector (EE) position (m)	0.1
Initial and final robot base contact position (m)	0.675
Vertical final hand and EE position (m)	0.6
Horizontal final hand and EE position (m)	0.3
Standing distance, $L$ (m)	1.3
$T$ (s)	1.2

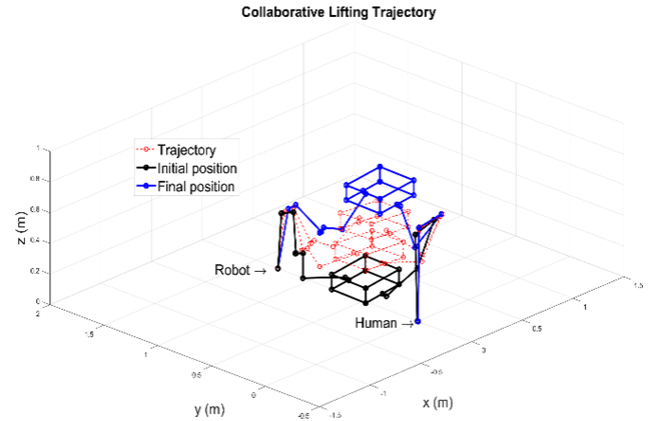


FIGURE 3: SNAPSHOTS OF HUMAN-ROBOT LIFTING MOTION FOR 10 KG BOX

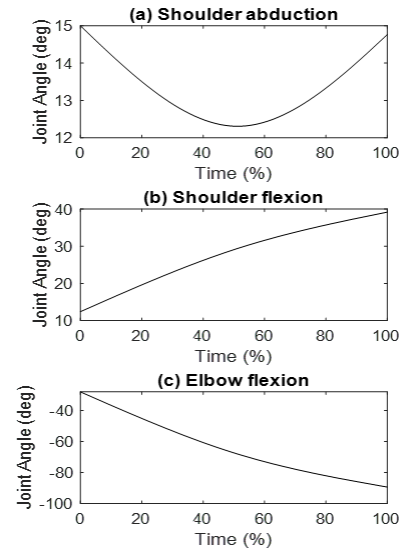


FIGURE 4: HUMAN ARM JOINT ANGLE PROFILES

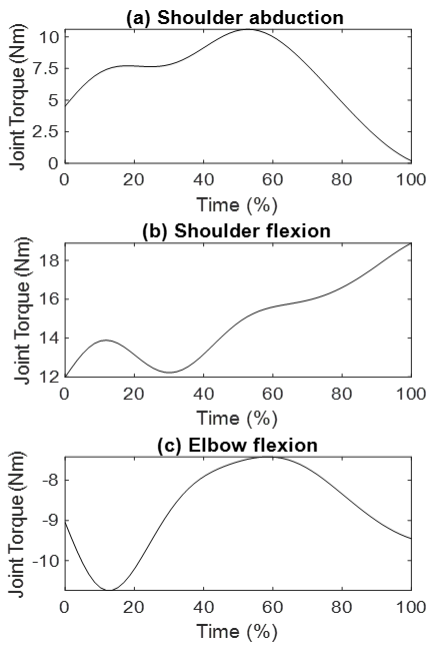


FIGURE 5: HUMAN ARM JOINT TORQUE PROFILES

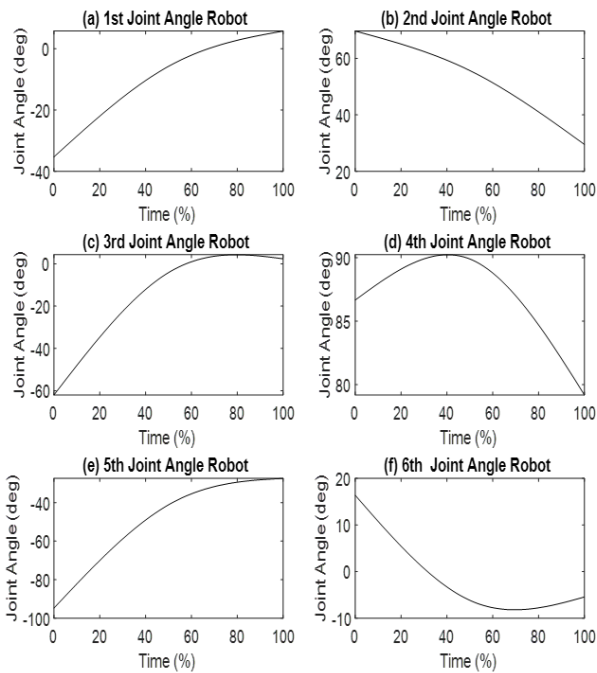


FIGURE 6: ROBOT ARM JOINT ANGLE PROFILES

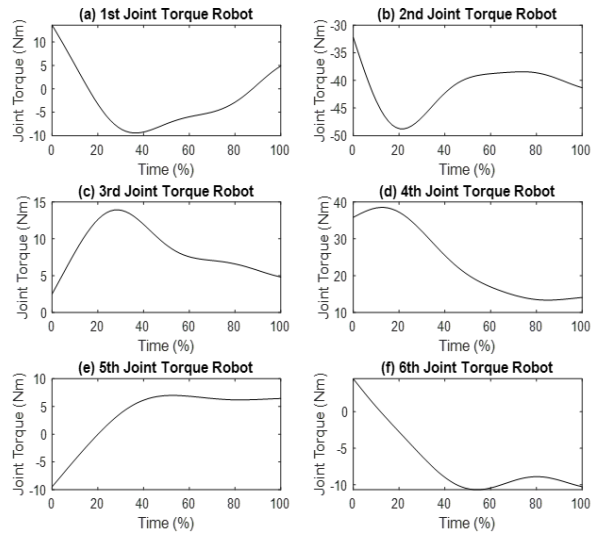


FIGURE 7: ROBOT ARM JOINT TORQUE PROFILES

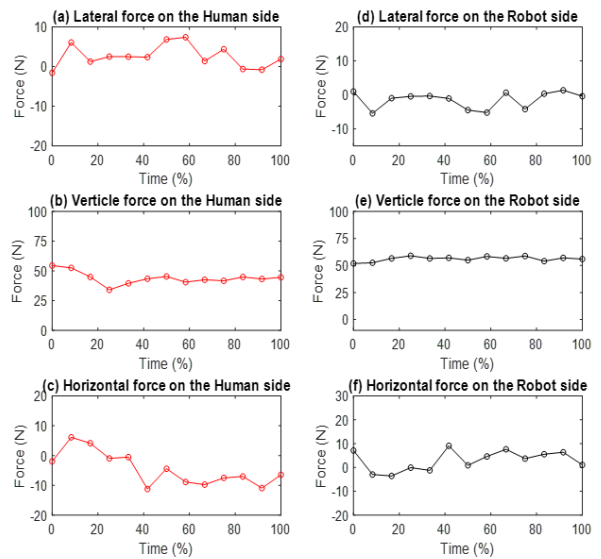


FIGURE 8: BOX GRASPING FORCES FOR HUMAN-ROBOT LIFTING

## 5. DISCUSSION

The trajectory of the simulated human-robot lifting motion is depicted in Figure 3. It is seen that the initial and final box locations are not symmetric because of the given final box location. The proposed optimization is able to predict a natural collaborative lifting motion. The joint angle profiles of shoulder flexion and elbow flexion of the human arm have similar trends as shown in Figure 4. In addition, the joint torque profile of shoulder flexion has a larger peak value than those of other joints as shown in Figure 5.

For robot joint angle profiles in Figure 6, all the joints have similar trends. These joint angle profiles indicate that all the rotational joints of the robot have effects on the collaborative lifting. The 2<sup>nd</sup> and 4<sup>th</sup> joints of the robot have larger peak torque values than those of other joints as depicted in Figure 7. This illustrates that every robot joint has different contribution to the box lifting. In addition, we need to validate the simulation results against the experimental results for robot joint angle profiles and joint torque profiles as presented in Figure 6 and Figure 7, respectively.

For box grasping forces, lateral and horizontal grasping forces have similar magnitudes but in the opposite directions to keep the box in balance as shown in Figure 8. In addition, the summation of the vertical grasping forces on both sides are approximately equal to the weight of the box.

## 6. CONCLUSION

In this study, an inverse dynamic optimization formulation was proposed to predict human-robot lifting motion and the grasping forces. Reasonable simulation results were obtained. DH method and recursive Lagrangian dynamics were used to calculate the kinematics and dynamics of the mechanical system of human-robot and box. The discretized grasping forces were used to model human-robot and box interaction. The NLP optimization problem was efficiently solved using a gradient-based optimizer SNOPT. These results can be used to plan the optimal human-robot collaborative lifting motion to prevent human injury. For future work, we will first validate the simulation results using motion captures, then design a lifting database for different box weights like in the literature for human team lifting [17]. This database can generate an efficient lifting motion for different box weights and locations for human-robot manipulations.

## ACKNOWLEDGEMENTS

This work is supported by NSF project (Award # 1849279).

## REFERENCES

[1] Ayoub, M., 1992, Problems and solutions in manual materials handling: the state of the art. *Ergonomics*, 35(7-8), 713-728.

[2] Arisumi, H., Chardonnet, J. R., Kheddar, A., and Yokoi, K., 2007, Dynamic lifting motion of humanoid robots, 2007 IEEE International Conference on Robotics and Automation, Roma, Italy, pp. 2661-2667.

[3] Xiang, Y., Arora, J.S., and Abdel-Malek, K., 2010, Physics-based modeling and simulation of human walking: a review of optimization-based and other approaches. *Structural and Multidisciplinary Optimization*, 42(1), 1-23.

[4] Xiang, Y., Arora, J.S., Rahmatalla, S., Marler, T., Bhatt, R., Abdel-Malek, K., 2010, Human lifting simulation using a multi-objective optimization approach, *Multibody System Dynamics*, 23(4), 431-451.

[5] Xiang, Y., Arora, J.S., & Abdel-Malek, K. 2012, 3D human lifting motion prediction with different performance measures. *International Journal of Humanoid Robotics*, 9(02), 1250012.

[6] Song, J., Qu, X., & Chen, C.H., 2016. Simulation of lifting motions using a novel multi-objective optimization approach. *International Journal of Industrial Ergonomics*, 53, 37-47.

[7] Xiang, Y., Arefeen, A. 2020, Two-dimensional team lifting prediction with floating-base box dynamics and grasping force coupling. *Multibody System Dynamics*, 50, 211–231.

[8] Sheng, W., Thobbi, A., and Gu, Y., 2015, An integrated framework for human-robot collaborative manipulation, *IEEE Transactions on Cybernetics*, 45(10), 2030-2041.

[9] Evrard, P., Gribovskaya, E., Calinon, S., Billard, A., and Kheddar, A., 2009, Teaching physical collaborative tasks: object-lifting case study with a humanoid," 2009 9th IEEE-RAS International Conference on Humanoid Robots, Paris, France, pp. 399-404, doi: 10.1109/ICHR.2009.5379513.

[10] DelPreto, J., and Rus, D., 2019, Sharing the load: human-robot team lifting using muscle activity, in 2019 IEEE International Conference on Robotics and Automation (ICRA), May 20-24, Montreal, Canada.

[11] Gill, P.E., Murray, W., and Saunders, M.A., 2002, SNOPT: An SQP algorithm for large-scale constrained optimization. *SIAM Journal of Optimization*, 12(4), 979-1006.

[12] Denavit, J., and Hartenberg, R.S., 1955, A kinematic notation for lower-pair mechanisms based on matrices, *Journal of Applied Mechanics*, 22, 215-221.

[13] Cheng, H., Obergefell, L., and Rizer, A., 1994, Generator of body (GEBOD) manual, AL/CF-TR-1994-0051, Armstrong Laboratory, Wright-Patterson Air Force Base, Ohio.

[14] Wang Y., Kong X., Yang J., Zhao G., 2020, Motion Performance Analysis of the Sawyer Ankle Rehabilitation Robot. In: Tan J. (eds) *Advances in Mechanical Design. ICMD 2019. Mechanisms and Machine Science*, vol 77. Springer, Singapore.

[15] Xiang, Y., Arora, J.S., Abdel-Malek, K., 2009. Optimization-based motion prediction of mechanical systems: a sensitivity analysis. *Structural and Multidisciplinary Optimization*, 37(6), 595-608.

[16] Xiang, Y., Arora, J.S., Rahmatalla, S., Abdel-Malek, K., 2009. Optimization-based dynamic human walking prediction: one step formulation. *International Journal for Numerical Methods in Engineering*, 79(6), 667-695.

[17] Arefeen, A., Xiang, Y., 2020, Two-dimensional team lifting prediction with different box weights. *Proceedings of the ASME 2020 International Design Engineering Technical Conferences and Computers and Information in Engineering Conference*. Volume 9: 40th Computers and Information in Engineering Conference (CIE). Virtual, Online. August 17–19, 2020. V009T09A004. ASME.